

## 一种吡啶三唑修饰的香豆素类荧光探针对 Cu<sup>2+</sup>的选择性识别

胡斌<sup>1,2</sup> 张益<sup>1</sup> 朱琳<sup>1</sup> 罗旭彪<sup>\*1</sup> 周丹<sup>1</sup> 谢宇<sup>1</sup> 黄伟<sup>\*2</sup>  
(<sup>1</sup>南昌航空大学,江西省持续性污染物控制与资源循环利用重点实验室,南昌 330063)  
(<sup>2</sup>南京大学化学化工学院,配位化学国家重点实验室,南京 210093)

**摘要:** 成功设计且合成了一个基于吡啶三唑修饰的香豆素席夫碱荧光探针 **CPTH**。分别利用 <sup>1</sup>H NMR、<sup>13</sup>C NMR、FT-IR 和 LC/MS 对其进行了表征。**CPTH** 在溶液中发射出强烈的黄色荧光并对铜离子表现出快速、优良的选择响应性。同时,**CPTH** 的灵敏度较高,其检出限低至 2 μmol·L<sup>-1</sup>。

**关键词:** 铜离子; 香豆素; 席夫碱; 荧光探针

中图分类号: O614.121 文献标识码: A 文章编号: 1001-4861(2020)07-1375-08

DOI: 10.11862/CJIC.2020.146

### A Pyridine Triazole Modified Coumarin Fluorescent Sensor for Selective Detection of Cu<sup>2+</sup> Ions

HU Bin<sup>1,2</sup> ZHANG Yi<sup>1</sup> ZHU Lin<sup>1</sup> LUO Xu-Biao<sup>\*1</sup> ZHOU Dan<sup>1</sup> XIE Yu<sup>1</sup> HUANG Wei<sup>\*2</sup>  
(*Key Laboratory of Jiangxi Province for Persistent Pollutants Control and Resources Recycle, Nanchang Hangkong University, Nanchang 330063, China*)  
(*State Key Laboratory of Coordination Chemistry, School of Chemistry and Chemical Engineering, Nanjing University, Nanjing 210093, China*)

**Abstract:** A coumarin Schiff-base fluorescent sensor bearing 2-(5-(pyridine-3-yl)-4H-1,2,4-triazol-3-yl)acetohydrazide unit (**CPTH**) was designed, synthesized and characterized. **CPTH** exhibited strong yellow fluorescence and unique selectivity for Cu<sup>2+</sup> ions. As a Cu<sup>2+</sup> ion quencher, **CPTH** showed highly sensitive detection limit of 2 μmol·L<sup>-1</sup>. CCDC: 1967788, **CPTH**.

**Keywords:** Cu<sup>2+</sup>; coumarin; Schiff-base; fluorescent probe

It has been well-known to us that certain metal ions play an indispensable role in animals, plants and humans of nature. For example, copper is the third richest metal element in our body (after zinc and iron) and essential trace elements for life activities. Lack of copper in the human body can cause anemia, abnormal hair, arteries, and even brain disorders<sup>[1-2]</sup>. However, excess of copper ions will cause severe neurodegenera-

tive diseases like Wilson disease<sup>[3]</sup>, Alzheimer's disease<sup>[4]</sup>, hypopigmentation, bone abnormalities. In addition, excessive copper as a pollutant causes a huge threat to the environment and ecosystem. The World Health Organization (WHO) determined copper ion as one of the most concerning chemical elements in drinking water. The United States Environmental Protection Agency (USEPA) has set the minimum detection limit

收稿日期: 2019-11-27。收修改稿日期: 2020-01-20。

国家自然科学基金(No. 21501088, 51678285, 1667019, 51703091, 21871133)、江西省优势科技创新团队建设计划项目(No.20165BCB19008)和江西省自然科学基金(No.20171ACB20016)资助。

\*通信联系人。E-mail: luoxubiao@126.com, whuang@nju.edu.cn

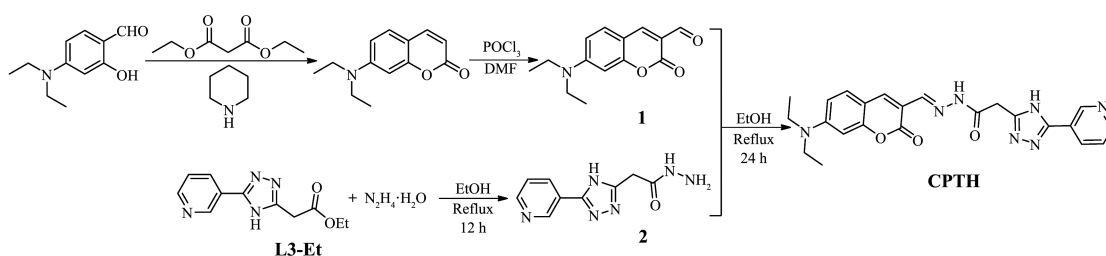
of copper ion in potable water to  $20 \mu\text{mol}\cdot\text{L}^{-1}$ <sup>[5]</sup>. For this reason, sensitive, selective and biocompatible approaches for the detection of copper ions are important from an environmental or biological perspective.

There are many traditional analytical techniques for detecting copper ions. For example, atomic emission and absorption spectrometry<sup>[6-7]</sup>, mass spectrometry<sup>[8]</sup> are widely used in recent years. However, the above-mentioned methods have obvious shortcomings, such as high-cost, tedious sample preparation procedures, and susceptible to interference from other ions. Alternatively, the fluorescent sensors with high selectivity, real-time detection and low detection limits<sup>[9-14]</sup> for various heavy metal ions stand out and have received increasing attention recently.

A great deal of fluorescent sensors, derived from rhodamine, coumarin, and 1,8-naphthalimide, *etc.*, have been documented for detecting copper ions<sup>[15-16]</sup>. Among them, some rhodamine or 1,8-naphthalimide-based probes are reported with some shortcomings. For example, rhodamine-based probes have shown poor selectivity, interfering with other transition metals such as  $\text{Co}^{2+}$ <sup>[17]</sup> and  $\text{Fe}^{3+}$ <sup>[18]</sup>. 1,8-Naphthalimide-based fluorescent probes may have high detection limits while their linear range is not clear enough<sup>[19]</sup>. In contrast, coumarin derivatives possess a series of excellent fluorescence properties, including photostability, low cytotox-

icity, large Stokes displacement and high fluorescence quantum yield<sup>[20-25]</sup>, and they have been inclusively utilized to prepare fluorescent sensors for the identification of various heavy metal ions. However, most of the known coumarin fluorescent probes face the problems of selectivity, sensitivity and biocompatibility<sup>[26-27]</sup>. It still remains a challenge to develop novel coumarin fluorescent probes for recognizing heavy metal ions with excellent selectivity, low detection limit and fast response time.

In this work, we try to combine the pyridine triazole (2-(5-(pyridine-3-yl)-4H-1,2,4-triazol-3-yl)acetylhydrazide) and coumarin moieties via a Schiff-base bridge to build a **CPTH** molecule with rich coordination sites and extended  $\pi$ -system (Scheme 1). And then, the photochemical properties and possible fluorescent sensors for certain metal ions have been explored for this coumarin derivative. The designed **CPTH** exhibited strong yellow fluorescence (excitation: 470 nm, emission: 520 nm), and the fluorescence was quenched quickly by adding copper ions. The detection limit of **CPTH** was found as low as  $2 \mu\text{mol}\cdot\text{L}^{-1}$ , which is analogous to highly sensitive coumarin-based chemosensors<sup>[26]</sup>. Moreover, **CPTH** showed a high selectivity for  $\text{Cu}^{2+}$  without interfered by many other common metal ions.



Scheme 1 Synthesis of **CPTH**

## 1 Experimental

Materials and measurement methods can be found in Support information.

### 1.1 Synthetic procedures

#### 1.1.1 Synthesis of compound 2

Compound **L3-Et** (0.232 g, 1.0 mmol) and hydra-

zine hydrate (0.1 mL, 80% concentrated, 1.64 mmol) was added in absolute ethanol (20 mL). The solution was mixed together and refluxed well at 80 °C overnight until TLC demonstrated the finish of the reaction, then a portion of solvent was evaporated and concentrated under vacuum condition by rotary evaporator. The obtained crude product was precipitated and fil-

tered from the remaining solvent, then recrystallized from absolute ethanol to get white powder of **2** (0.175 g, Yield: 82%). m.p. 150~151 °C. <sup>1</sup>H NMR (400 MHz, DMSO-d<sub>6</sub>): δ 9.47 (s, 1H), 9.15 (dd, *J*=2.2, 0.8 Hz, 1H), 8.81 (dd, *J*=4.8, 1.6 Hz, 1H), 8.50~8.20 (m, 1H), 7.65 (m, 1H), 4.38 (s, 2H), 3.92 (s, 2H). <sup>13</sup>C NMR (101 MHz, DMSO-d<sub>6</sub>): δ 165.0, 163.2, 163.1, 153.0, 147.5, 134.6, 124.9, 120.4, 31.4. LC/MS: *m/z*=242.25 for [M+Na]<sup>+</sup>. FT-IR (KBr, cm<sup>-1</sup>): 3 382 (m), 3 276 (s), 3 177 (w), 1 661 (vs), 1 526 (m), 1 411 (s), 1 247 (w), 1 015 (m). Anal. Calcd. for C<sub>9</sub>H<sub>10</sub>N<sub>6</sub>O(%): C, 49.54; H, 4.62; N, 38.51. Found(%): C, 49.38; H, 4.88; N, 38.27.

### 1.1.2 Synthesis of CPTH

Compound **1** (0.245 g, 1.0 mmol) and compound **2** (0.218 g, 1.0 mmol) in absolute ethanol (20 mL) was mixed and stirred at 80 °C for 24 h until the TLC showed the reaction was almost finished. The obtained yellow solution was cooled to room temperature and yellow solid was precipitated and filtered from the solution. The obtained crude product was recrystallized from ethanol to give orange powder of **CPTH** (0.356 g, Yield: 80%). m.p. 234~235 °C. <sup>1</sup>H NMR (400 MHz, DMSO-d<sub>6</sub>): δ 11.83 (s, 1H), 9.19 (s, 1H), 8.82 (dd, *J*=4.8, 1.7 Hz, 1H), 8.42~8.36 (m, 1H), 8.34 (s, 1H), 8.08 (s, 1H), 7.66 (m, 1H), 7.48 (d, *J*=9.0 Hz, 1H), 6.76 (dd, *J*=9.0, 2.3 Hz, 1H), 6.58 (d, *J*=2.2 Hz, 1H), 4.56 (s, 2H), 4.13 (s, 1H), 3.47 (q, *J*=6.8 Hz, 4H), 1.14 (t, *J*=7.0 Hz, 6H). <sup>13</sup>C NMR (101 MHz, DMSO-d<sub>6</sub>): δ 167.0, 163.6, 162.0, 161.6, 157.1, 152.4, 151.8, 147.9, 140.4, 139.3, 134.3, 130.5, 123.8, 120.4, 112.3, 109.8, 108.6, 97.2, 45.1, 31.4, 29.7, 12.5. LC/MS: *m/z*=447.20 for [M+H]<sup>+</sup>, *m/z*=469.20 for [M+Na]<sup>+</sup>. FT-IR (KBr, cm<sup>-1</sup>): 2 974 (vw), 1 691 (vs), 1 627 (s), 1 602 (vs), 1 579 (m), 1 361 (w), 1 348 (w), 1 261 (m). Anal. Calcd. for C<sub>23</sub>H<sub>23</sub>N<sub>7</sub>O<sub>3</sub>(%): C, 62.01; H, 5.20; N, 22.01. Found(%): C, 61.90; H, 5.27; N, 21.87. Single crystals of CPTH suitable for X-ray diffraction measurement were obtained by slow evaporation of a mixture of CHCl<sub>3</sub> in air for one week.

CCDC: 1967788, **CPTH**.

## 1.2 UV-Vis and fluorescence spectra of CPTH

The spectral analyses were done in a H<sub>2</sub>O-DMF PBS buffer (phosphate buffer saline) (10 mmol·L<sup>-1</sup>, pH

=7.40, 1:9, V/V) solution at 25 °C. The concentration of CPTH was 10 μmol·L<sup>-1</sup>. Solutions of Ag<sup>+</sup>, Al<sup>3+</sup>, Ba<sup>2+</sup>, Cd<sup>2+</sup>, Ca<sup>2+</sup>, Co<sup>2+</sup>, Cu<sup>2+</sup>, Cr<sup>3+</sup>, Fe<sup>2+</sup>, Fe<sup>3+</sup>, K<sup>+</sup>, Hg<sup>2+</sup>, Mg<sup>2+</sup>, Mn<sup>2+</sup>, Na<sup>+</sup>, Zn<sup>2+</sup> and Pb<sup>2+</sup> ions were prepared with nitrate or acetate salts in water. The excitation wavelength was 470 nm and the fluorescence emission spectra were recorded within the scope of 480~650 nm.

## 2 Results and discussions

### 2.1 Synthesis

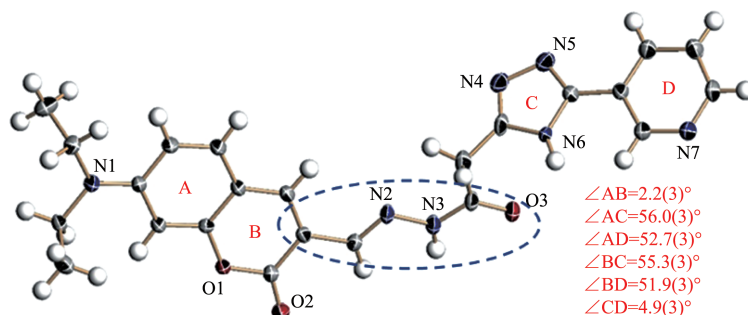
The coumarin unit was first combined with the pyridine triazole unit to construct a new fluorescent sensor **CPTH**. As shown in Scheme 1, **CPTH** was prepared with a satisfactory yield through the imine condensation reaction between precursors **1** and **2** under the refluxing condition. The successful preparation of **CPTH** was confirmed by <sup>1</sup>H/<sup>13</sup>C NMR, FT-IR and ESI-MS. It is worth noting that the single peak of the aldehyde proton in compound **1** at δ 10.13 disappeared after the Schiff-base condensation and the two amine protons of azine group at δ 3.92 were gone in the other starting compound **2** simultaneously. Instead, a new single peak at δ 7.66 was observed in **CPTH**, indicative of the formation of imine unit. At the same time, two methylene protons were low-field shifted from δ 4.38 to 4.56 in **2** and **CPTH**. In addition, an LC/MS peak of **CPTH** was found at *m/z*=447.20 with the 100% abundance corresponding to the expected molecular ion peak. FT-IR spectral comparisons revealed the disappearance of 1 677 cm<sup>-1</sup> in **1**, 3 382 and 3 276 cm<sup>-1</sup> in **2**, and the emergence of 1 627 cm<sup>-1</sup> in **CPTH**, corresponding to the functional radical transformation from aldehyde and amine to imine groups. Meanwhile, the absorption peak for carbonyl group of coumarin unit was shifted from 1 717 cm<sup>-1</sup> in **1** to 1 691 cm<sup>-1</sup> in **CPTH** after the Schiff-base condensation, which was consistent with the alteration of force constant (*k*) for C=O and C=N bonds.

### 2.2 Structural description of compound CPTH

In order to further characterize our compound **CPTH**, its single-crystal structure has been successfully acquired. The molecular structure of **CPTH** with atom-numbering schemes is shown in Fig.1 and details

of the data collection and refinement results are listed in Table 1. **CPTH** crystallizes in the orthorhombic *Pbcn* space group without the presence of any solvent molecule. The dihedral angles between the aromatic rings at both ends of **CPTH** are small, and the planarity of coumarin moiety can be extended to the carbonyl oxygen atom of the hydrazide unit. The central six non-hydrogen atoms (C<sub>3</sub>N<sub>2</sub>O) circled in Fig.1 have the mean deviation of 0.002 4(4) nm from the least-squares plane. However, the  $\pi$ -conjugated system is destroyed

by the presence of an  $sp^3$  carbon atom linked to the triazole ring. This structural feature is consistent with the UV-Vis spectrum of **CPTH**, as illustrated in Fig.S11. In the crystal structure of **CPTH**, an offset dimeric packing mode is observed with a head-to-tail manner, as displayed in Fig.2, where strong  $\pi$ - $\pi$  stacking interactions are discovered between adjacent benzene and pyrone rings of coumarin moiety with the centroid-centroid separation of 0.379(1) nm. In addition, every dimeric pair is linked with four close dimeric units via



Displacement ellipsoids are drawn at the 30% probability level and the H atoms are shown as small spheres of arbitrary radii

Fig.1 ORTEP drawing of compound **CPTH** with the atom-numbering scheme

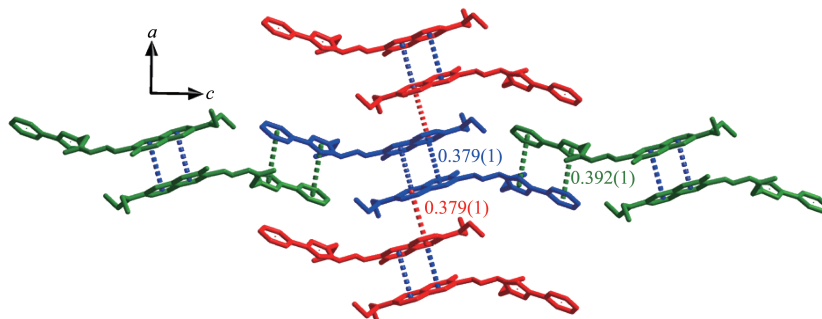


Fig.2 Perspective view of the crystal packing of compound **CPTH** with the labeling of  $\pi$ - $\pi$  stacking interactions

Table 1 Crystal structural refinement details for compound **CPTH**

Empirical formula	C <sub>23</sub> H <sub>23</sub> N <sub>7</sub> O <sub>3</sub>	$D_c / (\text{g} \cdot \text{cm}^{-3})$	1.389
Formula weight	445.48	$F(000)$	1 872
Temperature / K	190(2)	$\mu / \text{mm}^{-1}$	0.096
Wavelength / nm	0.071 07	$h_{\min}, h_{\max}$	-9, 9
Crystal size / mm	0.10×0.10×0.11	$k_{\min}, k_{\max}$	-15, 10
Crystal system	Orthorhombic	$l_{\min}, l_{\max}$	-43, 47
Space group	<i>Pbcn</i>	Data, parameter	3 885, 304
$a / \text{nm}$	0.820 6(3)	Final $R$ indices [ $I > 2\sigma(I)$ ]*	$R_1=0.060$ 0, $wR_2=0.151$ 7
$b / \text{nm}$	1.312 8(4)	$R$ indices (all data)	$R_1=0.115$ 9, $wR_2=0.185$ 0
$c / \text{nm}$	3.955 5(14)	$S$	1.023
$V / \text{nm}^3$	4.261(3)	$(\Delta\rho)_{\max}, (\Delta\rho)_{\min} / (\text{e} \cdot \text{nm}^{-3})$	437, -544
$Z$	8		

\* $R_1 = \sum \|F_o\| - |F_c\| / \sum \|F_o\|$ ,  $wR_2 = \{ \sum [w(F_o^2 - F_c^2)^2] / \sum w(F_o^2) \}^{1/2}$

two types of weaker  $\pi$ - $\pi$  stacking interactions. One comes from neighboring coumarin benzene rings with the longer centroid-centroid distance of 0.397(1) nm, and the other stems from adjacent protruding triazole and pyrimidine rings with double complementary  $\pi$ - $\pi$  stacking interactions (0.392(1) nm).

### 2.3 Spectral characterizations

As shown in Fig. S11, the maximum absorption wavelength of compound **1** was located at 449 nm, indicative of the  $\pi$ -conjugated system of coumarin backbone. In contrast, no obvious absorption peak was found in **2** revealing the lack of extended  $\pi$ -system within the molecule. After the imine condensation, the maximum absorption wavelength of **CPTH** was the same as that of **1**, indicating their analogous  $\pi$ -conjugated skeleton just by changing the heteroatoms from O to N.

Since **CPTH** has multiple coordinating sites, we tried to explore its coordination with common metal ions. As shown in Fig.3, when **CPTH** was mixed with Cu<sup>2+</sup> ions, the maximum absorption wavelength was bathochromically shifted to 475 nm, whereas the addition of the other metal ions had no evident impact on the resultant absorption peak. Considering the presence of fluorescence active coumarin moiety, fluorescence spectrum was further studied for the interactions between this **CPTH** molecule and a variety of metal

ions.

The rigid planar structure of the coumarin molecule gave it a large conjugated  $\pi$  bond, so most of the coumarin derivatives had fluorescence. As shown in Fig.4, **CPTH** exhibited very strong yellow fluorescence ( $\lambda_{\text{ex}}=480$  nm,  $\lambda_{\text{em}}=520$  nm) in the buffered DMF/PBS (10 mmol·L<sup>-1</sup>, pH=7.40, 1:9, V/V) solution, which was similar to those reported in literature<sup>[28]</sup>. After the addition of 1.0 equiv. of Cu<sup>2+</sup>, the fluorescence of **CPTH** was instantly quenched. However, the addition of other common metal ions had no effect on the fluorescence spectrum of **CPTH**, suggesting excellent selectivity of **CPTH** to copper ions. The fluorescence quenching phenomenon may be ascribed to the selective combination of **CPTH** with Cu<sup>2+</sup> ion<sup>[29-32]</sup>.

The above experimental results showed that **CPTH** may have potential applications in the selective identification of copper ions, so the disturbance of other coexistent heavy metal cations was also carried out (Fig. 5a). **CPTH** (20  $\mu\text{mol}\cdot\text{L}^{-1}$ ) was mixed with 2.0 equiv. of Cu<sup>2+</sup> in the presence of 2.0 equiv. of other common metal cations (Ag<sup>+</sup>, Al<sup>3+</sup>, Ba<sup>2+</sup>, Cd<sup>2+</sup>, Ca<sup>2+</sup>, Co<sup>2+</sup>, Cu<sup>2+</sup>, Cr<sup>3+</sup>, Fe<sup>2+</sup>, Fe<sup>3+</sup>, K<sup>+</sup>, Hg<sup>2+</sup>, Mg<sup>2+</sup>, Mn<sup>2+</sup>, Na<sup>+</sup>, Zn<sup>2+</sup> and Pb<sup>2+</sup> ions). The results displayed that the coexisting metal ions had negligible effects on the fluorescence quenching of **CPTH**, indicating excellent selective detection of Cu<sup>2+</sup> under physiological conditions.

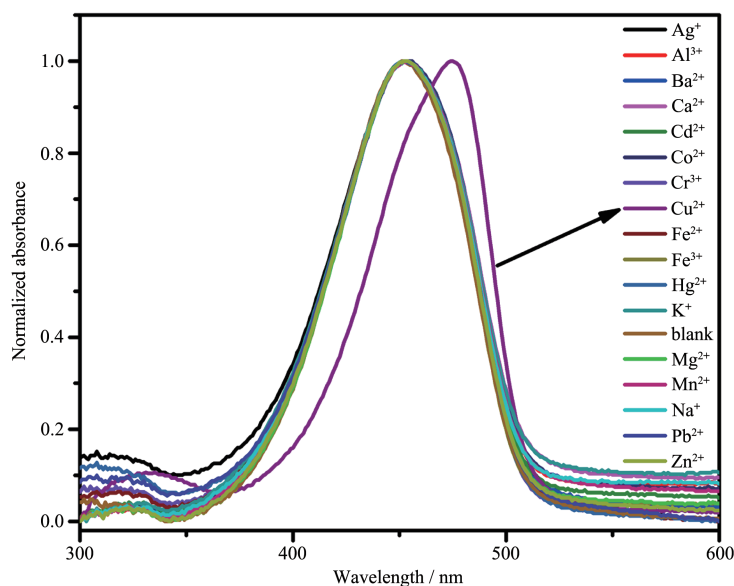
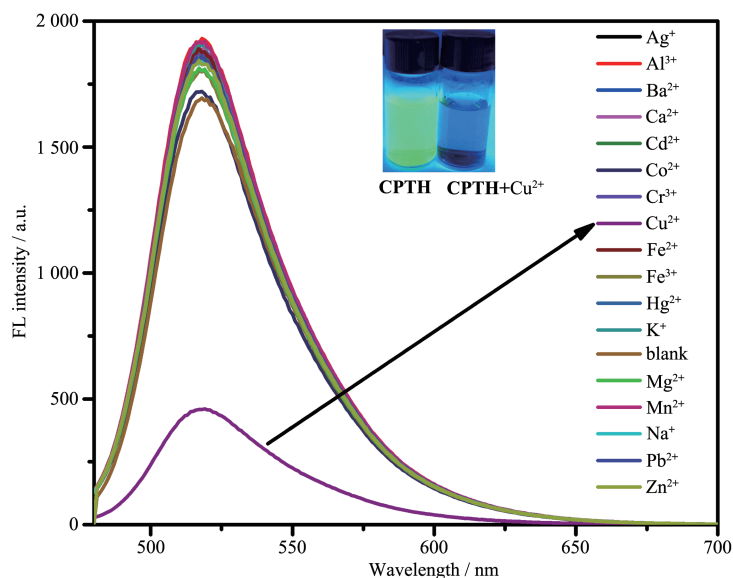
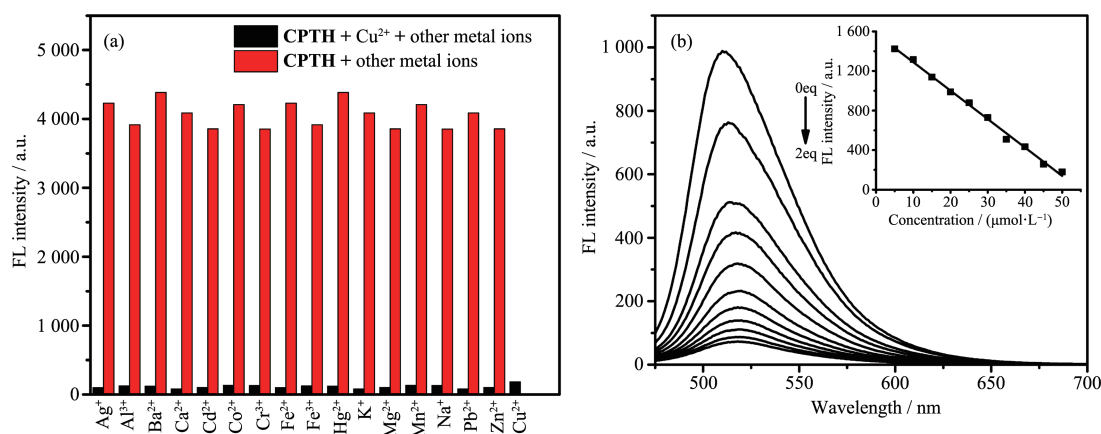


Fig.3 UV-Vis spectra of **CPTH** (10  $\mu\text{mol}\cdot\text{L}^{-1}$ ) after adding different metal ions



Excitation wavelength was 470 nm; Inset: digital photo showing the fluorescence color of **CPTH** and **CPTH** with  $\text{Cu}^{2+}$

Fig.4 Fluorescence emission spectra of **CPTH** ( $10 \mu\text{mol}\cdot\text{L}^{-1}$ ) after adding different metal ions



Inset: fluorescence at 520 nm as a function of  $\text{Cu}^{2+}$  ion concentration

Fig.5 (a) Fluorescence quenching response of **CPTH** ( $20 \mu\text{mol}\cdot\text{L}^{-1}$ ) towards  $\text{Cu}^{2+}$  (2.0 equiv.) in the presence of other metal cations (2.0 equiv.); (b) Fluorescence spectra titration of **CPTH** ( $5 \mu\text{mol}\cdot\text{L}^{-1}$ ) upon addition of  $\text{Cu}^{2+}$

In order to assess the sensitivity limit of **CPTH** for  $\text{Cu}^{2+}$  detection, fluorescence spectral titrations were implemented. As depicted in Fig.5b, the fluorescence intensity of the peak of **CPTH** ( $5 \mu\text{mol}\cdot\text{L}^{-1}$ ) at 520 nm gradually decreased with the increase of  $\text{Cu}^{2+}$  concentration (from 0 to 2.0 equiv.), indicating concentration dependent fluorescence quenching. This observation can be explained by the formation of **CPTH**- $\text{Cu}^{2+}$  complex. The detection limit of **CPTH** for  $\text{Cu}^{2+}$  was calculated to be  $2 \mu\text{mol}\cdot\text{L}^{-1}$ , which was gotten by the linear fitting of  $\text{Cu}^{2+}$  concentrations from 10 to  $50 \mu\text{mol}\cdot\text{L}^{-1}$  (Inset of Fig.5b). Specifically, the detection limit was

calculated according to the formula of  $\text{LOD}=3\sigma/k$ , where  $k$  is the slope of the linear equation of  $y=kx+b$  between fluorescence intensity and concentration. The detection limit of **CPTH** for copper ions was far below the standard limit ( $20 \mu\text{mol}\cdot\text{L}^{-1}$ ) for  $\text{Cu}^{2+}$  in potable water regulated by the USEPA<sup>[10]</sup>.

Job's plot was conducted to determine the stoichiometric ratio between  $\text{Cu}^{2+}$  and **CPTH**. The total concentration of  $\text{Cu}^{2+}$  and **CPTH** was  $10 \mu\text{mol}\cdot\text{L}^{-1}$ . As can be seen in Fig.6a, the inflection point was found approximately 0.5 molar fraction indicating a 1:1 stoichiometric ratio between  $\text{Cu}^{2+}$  and **CPTH**. It could be

further confirmed by an ESI-MS peak at  $m/z=509.42$  (Fig.SI10) with the 100% abundance, corresponding to the molecular ion peak of  $[\text{Cu}^{2+}+\text{CPTH}]$  species. Based upon above-mentioned results and the molecular structure of **CPTH**, it is deduced that **CPTH** serves as a tridentate ligand to coordinate with  $\text{Cu}^{2+}$  in the 1:1 chelating fashion, where two fused five-membered ( $\text{CN}_2\text{OCu}$ ) and six-membered ( $\text{C}_3\text{NOCu}$ ) chelating rings are formed, as displayed in Scheme 2. In addition,  $\text{Cu}(\text{OAc})_2 \cdot \text{H}_2\text{O}$ ,  $\text{CuCl}_2 \cdot 2\text{H}_2\text{O}$ ,  $\text{Cu}(\text{ClO}_4)_2 \cdot 6\text{H}_2\text{O}$ ,  $\text{CuBr}_2$  and  $\text{Cu}(\text{NO}_3)_2 \cdot 3\text{H}_2\text{O}$  were used to explore the **CPTH**'s anti-interference ability to anions. The results were given in Fig.6b, in which the fluorescence quenching of **CPTH** was independent of the tested anions suggesting the strong anti-interference to anions for **CPTH**.

One of the main advantages of fluorescent probes for detecting metal ions compared to other traditional methods was their real-time detection. Thus, the impact of the reaction time on the binding efficiency of  $\text{Cu}^{2+}$  ion to **CPTH** was investigated. As pictured in Fig. SI2. After the adding of 1.0 equiv.  $\text{Cu}^{2+}$  ion to **CPTH** solution ( $5 \mu\text{mol} \cdot \text{L}^{-1}$ ), the fluorescence intensity of **CPTH** reached a stable value within 5 s and kept unchangeable from 5 to 120 s. Thus, a reaction time was determined as 5 s in this probe detection system. Moreover, the effect of pH stability on **CPTH** was tested when interacting with copper ions, where the fluorescent probe **CPTH** showed a relatively wide pH value range of 4~7.5 for the detection of copper ions (Fig. SI3).

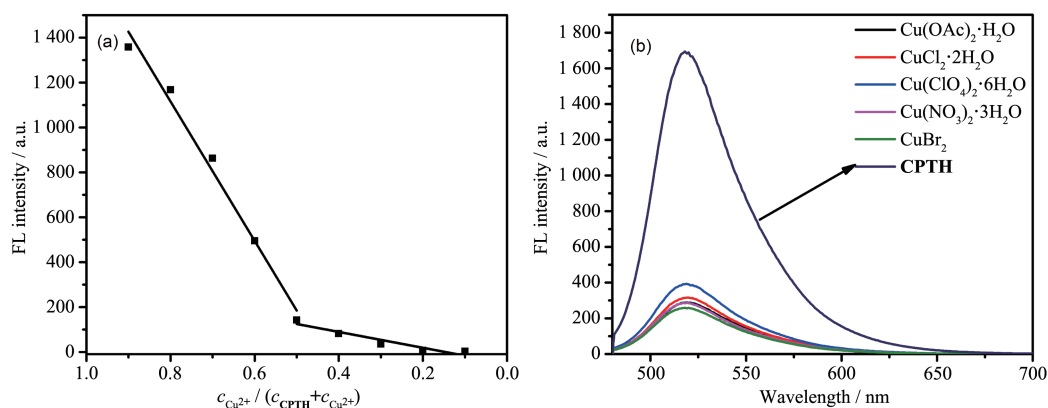
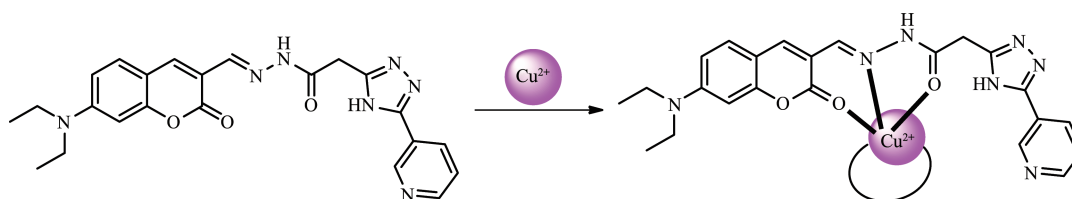


Fig.6 (a) Job's plot of the **CPTH**; (b) Fluorescence spectra of probe **CPTH** ( $10 \mu\text{mol} \cdot \text{L}^{-1}$ ) upon addition of different copper salts



Scheme 2 Possible coordination mode between **CPTH** and  $\text{Cu}^{2+}$  ion

### 3 Conclusions

In summary, the pyridine triazole unit was first used to construct a coumarin based fluorescent sensor via a simple synthetic approach. After the adding of  $\text{Cu}^{2+}$  ions, the maximum absorption wavelength of **CPTH** was red-shifted from 450 to 475 nm. And fluorescence quenching of **CPTH** was observed at 520 nm under the excitation of 470 nm, which did not take ef-

fect for other metal ions. Probe **CPTH** is highly selective for  $\text{Cu}^{2+}$  detection. This may be attributed to the fact that the Jahn-Teller deformation of  $\text{Cu}(\text{II})$  complexes provides excellent thermodynamic stability among all metal cations, so the  $d^9$  block metal  $\text{Cu}(\text{II})$  cation was preferentially used as the target ion during the metal transfer process. Job's plot revealed that the binding ratio of copper ion to probe **CPTH** is 1:1, which could be further confirmed by the presence of a molecular ion

peak for  $[\text{Cu}^{2+} + \text{CPTH}]$  species in ESI-MS. Copper ion detection limit of probe **CPTH** was measured to be  $2 \mu\text{mol} \cdot \text{L}^{-1}$ . Our contribution herein could provide certain new insights for exploring highly sensitive and selective coumarin based fluorescent sensors derived from aromatic heterocyclic Schiff base with multiple coordinating atoms.

Supporting information is available at <http://www.wjhxzb.cn>

## References:

- [1] Zhao H, Feng P, Cao J, et al. *Org. Biomol. Chem.*, **2012**, **10**: 3104-3109
- [2] Halfdanarson T R, Kumar N, Li R L, et al. *Eur. J. Haematol.*, **2008**, **80**:523-531
- [3] Bull P C, Thomas G R, Rommens J M, et al. *Nat. Genet.*, **1993**, **5**:323-337
- [4] Barnham K J, Masters C L, Bush A L, et al. *Nat. Rev. Drug Discov.*, **2004**, **3**:205-214
- [5] Chang H Q, Zhao X L, Wu W N, et al. *J. Lumin.*, **2017**, **182**: 268-273
- [6] Otero-Romani J, Moreda-Pineiro A, Bermejo-Barrera A, et al. *Anal. Chim. Acta*, **2005**, **536**:213-218
- [7] Gonzales A P S, Firmino M A, Nomura C S, et al. *Anal. Chim. Acta*, **2009**, **636**:198-204
- [8] Becker J S, Matusch A, Depboylu C, et al. *Anal. Chem.*, **2007**, **79**:6074-6080
- [9] Xu Z, Zhang L, Guo R, et al. *Sens. Actuators B*, **2011**, **156**:546-552
- [10] Xu Z H, Wang H W, Hou X F, et al. *Sens. Actuators B*, **2014**, **201**:469-474
- [11] Qin J C, Yang Z Y, Wang G Q, et al. *Tetrahedron Lett.*, **2015**, **56**:5024-5029
- [12] Qin J C, Yang Z Y, Wang G Q, et al. *J. Photochem. Photobiol. A*, **2015**, **310**:122-127
- [13] XU Fan(徐帆), WU Fang-Hui(吴芳辉), CHENG Li-Chun(程立春), et al. *J. Anal. Sci.*(分析科学学报), **2016**, **32**(3):335-339
- [14] QI Qi(齐琪), LI Xing(李星). *Chinese J. Inorg Chem.*(无机化学学报), **2019**, **35**(7):1301-1311
- [15] Xu J, Hou Y, Ma Q, et al. *Spectrochim. Acta A*, **2014**, **124**:416-422
- [16] ZHANG Chang-Li(张长丽), ZHANG Hong(张虹), HE Feng-Yun(何风云), et al. *Chinese J. Inorg Chem.*(无机化学学报), **2019**, **35**(10):1869-1876
- [17] Li C R, Yang Z Y, Li S R, et al. *J. Lumin.*, **2018**, **198**:327-336
- [18] Gahlyan P, Bawa R, Jain H, et al. *Chemistry Select*, **2019**, **4**: 7532-7540
- [19] Yuan L, Lin W, Chen B, et al. *Org. Lett.*, **2012**, **14**:432-435
- [20] Goswami S, Sen D, Das A K, et al. *Sens. Actuators B*, **2013**, **183**:518-525
- [21] Wang M, Wen J, Qin Z, et al. *Dyes Pigm.*, **2015**, **120**:208-212
- [22] Shiraiishi Y, Nakamura M, Hirai T, et al. *Phys. Chem. Chem. Phys.*, **2015**, **17**:25027-25036
- [23] Maiti S, Aydin Z, Zhang Y, et al. *Dalton Trans.*, **2015**, **44**: 8942-8949
- [24] He L, Lin W, Xu Q, et al. *Chem. Commun.*, **2015**, **51**:1510-1513
- [25] Kim K B, Kim H, Song E J, et al. *Dalton Trans.*, **2013**, **42**: 16569-16577
- [26] Wang S, Wang Z, Yin Y, et al. *J. Photochem. Photobiol. A*, **2017**, **333**:213-219
- [27] Mergu N, Kim M, Son Y A, et al. *Spectrochim. Acta A*, **2018**, **188**:571-580
- [28] Saini N, Prigyi N, Wannasiri C, et al. *J. Photochem. Photobiol. A*, **2018**, **358**:215-225
- [29] Borase P N, Thale P B, Shankarling G S, et al. *Dyes Pigm.*, **2016**, **134**:276-284
- [30] Huang L, Cheng J, Xie K, et al. *Dalton Trans.*, **2011**, **40**: 10815-10817
- [31] Yang W, Chen X, Su H, et al. *Chem. Commun.*, **2015**, **51**: 9616-9619
- [32] Su H, Chen X, Fang W, et al. *Anal. Chem.*, **2014**, **86**:891-899